Protein Science (1996), 5:341-347. Cambridge University Press. Printed in the USA.

Determinants of performance in the isocitrate dehydrogenase of *Escherichia coli*

ANTONY M. DEAN,[1] ANDREW K. SHIAU,[2,3] AND DANIEL E. KOSHLAND, JR.[2]

[1] Department of Biological Chemistry, The Chicago Medical School, 3333 Green Bay Road, North Chicago, Illinois 60064-3095
[2] Department of Molecular and Cell Biology, University of California, Berkeley, California 94720

(RECEIVED September 12, 1995; ACCEPTED November 28, 1995)

Abstract

The substrate specificity of the NADP-dependent isocitrate dehydrogenase of *Escherichia coli* was investigated by combining site-directed mutagenesis and utilization of alternative substrates. A comparison of the kinetics of the wild-type enzyme with 2R-malate reveals that the γ-carboxylate of 2R,3S-isocitrate contributes a factor of 12,000,000 to enzyme performance. Analysis of kinetic data compiled for 10 enzymes and nine different substrates reveals that a factor of 1,650 can be ascribed to the hydrogen bond formed between S113 and the γ-carboxylate of bound isocitrate, a factor of 150 to the negative charge of the γ-carboxylate, and a factor of 50 for the γ-methyl. These results are entirely consistent with X-ray structures of Michaelis complexes that show a hydrogen bond positions the γ-carboxylate of isocitrate so that a salt bridge can form to the nicotinamide ring of NADP.

Keywords: enzyme performance; isocitrate dehydrogenase; stabilization of Michaelis complex

The isocitrate dehydrogenase (IDH; 2R,3S-isocitrate:$NADP^+$ oxidoreductase [decarboxylating]; EC 1.1.1.42) of *Escherichia coli* catalyzes the oxidation of isocitrate to α-ketoglutarate and CO_2 using NADP as a coenzyme via a steady-state random kinetic mechanism (Dean & Koshland, 1993). The enzyme is inactivated by phosphorylation at S113 (Fig. 1A; Borthwick et al., 1984), an active site residue to which the γ-carboxylate of isocitrate normally hydrogen bonds (Hurley et al., 1990b). Kinetic analyses (Thorsness & Koshland, 1987; Dean & Koshland, 1990) and equilibrium binding experiments (Dean et al., 1989) confirm that the direct electrostatic repulsion of the γ-carboxylate by the phosphoserine is sufficient to inactivate IDH in the absence of major conformational changes (Hurley et al., 1990a).

The contributions to inactivation made by the phosphoserine have been mimicked by substituting various amino acids for S113. Alanine breaks the hydrogen bond to the γ-carboxylate of the substrate, causing a 1,000-fold reduction in performance (defined as $k_{cat}/K_{m\cdot\text{isocitrate}}/K_{m\cdot\text{NADP}}$); tyrosine causes a further 50-fold reduction, presumably as a consequence of steric effects; and aspartate and glutamate cause a dramatic 2,000,000-fold reduction (Thorsness & Koshland, 1987; Dean & Koshland, 1990) through electrostatic repulsion. As a control, the kinetics with 2R-malate, an alternative substrate that lacks the charged γ-carboxylate of isocitrate, were shown to be little influenced by substitutions at site 113 (Dean & Koshland, 1990). Intriguingly, however, 2R-malate is a very much poorer substrate for IDH than isocitrate.

Recently, the structures of a pseudo-Michaelis complex with both Ca^{2+}-isocitrate and NADP bound to the wild-type enzyme and a Laue structure of the Michaelis complex with Mg^{2+}-isocitrate and NADP bound to the K230M mutant enzyme have been determined (Stoddard et al., 1993; Bolduc et al., 1995). In both structures, the nicotinamide ring of the coenzyme lies immediately above isocitrate, with the C_4 carbon of the nicotinamide ring positioned to receive the α-carbon hydride from isocitrate on its *re*-face (Fig. 1B). In both structures a salt bridge forms between the positively charged nicotinamide ring and the negatively charged γ-carboxylate of the substrate, which also hydrogen bonds to the nicotinamide amide. There appear to be no other strong interactions; indeed, the entire nicotinamide mononucleotide moiety is disordered in the binary complex of wild-type IDH with NADP (Hurley et al., 1991).

To analyze the factors that determine enzyme performance, we have prepared nine mutants of the serine at position 113 and studied the kinetics toward the natural and eight alternative substrates.

Reprint requests to: Daniel E. Koshland, Jr., Department of Molecular and Cell Biology, University of California, Berkeley, California 94720; e-mail: daniel_koshland@maillink.berkeley.edu.

[3] Present address: Department of Biochemistry and Biophysics, University of California at San Francisco, San Francisco, California 94143.

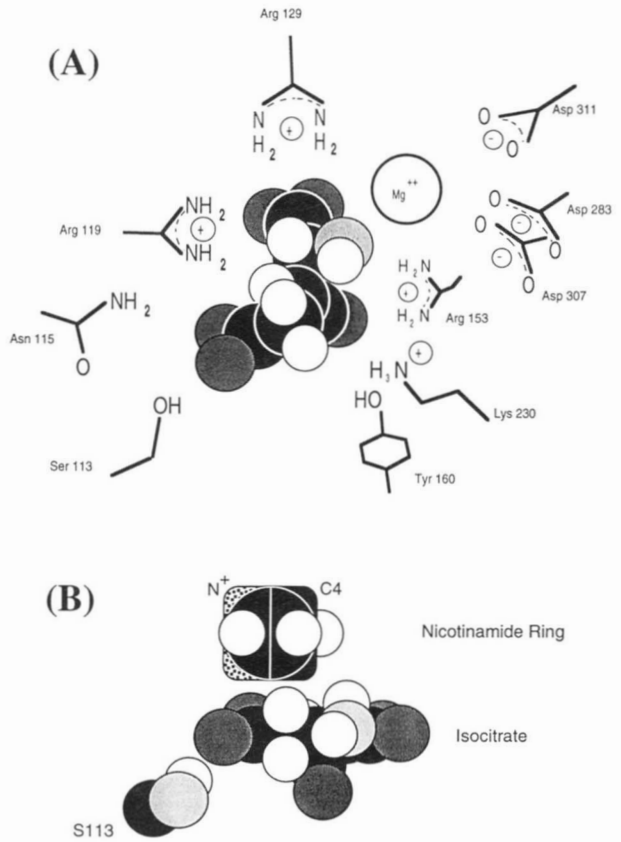

Fig. 1. A: Isocitrate binding site of IDH. Isocitrate (shaded spheres: carbon is black, hydrogen is white, charged oxygens are heavily shaded, uncharged oxygens are lightly shaded) binds between the two domains of IDH in a pocket formed from both subunits. R119, R129, and R153 form hydrogen bonds to the α- and β-carboxylates of isocitrate. The α-hydroxyl group and α-carboxylate of isocitrate are chelated to a magnesium ion associated with D283 and D307 and two active site waters (not shown) in a roughly octahedral manner. This structure is consistent with much previous work on the catalytic mechanism suggesting that dehydrogenation at the α-carbon precedes decarboxylation at the β-carbon (Hurley et al., 1991). D283 is suitably aligned to act as a catalytic base abstracting a proton from the α-hydroxyl during dehydrogenation, and K230 probably acts as the catalytic acid donating a proton to the β-carbon during decarboxylation. The γ-carboxylate moiety of isocitrate, which plays no direct chemical role in catalysis, forms a hydrogen bond to the serine at site 113, the site of phosphorylation, and may also interact electrostatically with N115. **B:** Detail of the structure of the IDH Michaelis complex. The nicotinamide ring lies immediately above isocitrate with its C_4 carbon positioned to receive the α-carbon hydride of the substrate on its *re*-face. The nicotinamide mononucleotide moiety of NADP is disordered in the binary complex (Hurley et al., 1990a, 1990b), allowing isocitrate to bind. The γ-carboxylate of isocitrate clearly forms a salt bridge to the charged nitrogen of the nicotinamide ring. The structure suggests that the salt bridge is crucial for a correct alignment of the nicotinamide ring for catalysis.

Results

The NADP Michaelis constants

When 2R,3S-isocitrate is utilized, the NADP Michaelis constants ($K_{m\cdot NADP}$) of all mutant enzymes are approximately 10-fold higher than that of the wild-type enzyme (Table 1). When 2R-malate, which lacks the γ-carboxylate of isocitrate, is utilized, the $K_{m\cdot NADP}$ of the wild-type enzyme is also 10-fold higher. Hence, the mere presence of a negative charge in the vicinity, introduced either as a γ-carboxylate on the substrate isocitrate or on the protein as an aspartate or a glutamate residue at site 113, need not reduce $K_{m\cdot NADP}$. This suggests that the hydrogen bond from S113 helps align the γ-carboxylate of isocitrate in a position suitable for salt bridge formation to the nicotinamide ring of NADP.

Table 1. *Maximum velocities and NADP Michaelis constants*[a]

	Substrate			
	Isocitrate		Malate	
Residue at site 113	k_{cat} (s^{-1})	K_m (μM)	k_{cat} (s^{-1})	K_m (μM)
Ala	2.2	260	1.2×10^{-3}	275
Asn	3.9	290	6.7×10^{-4}	230
Asp	3.3×10^{-2}	270	7.6×10^{-3}	326
Gln	1.0	230	4.1×10^{-4}	290
Glu	5.3×10^{-2}	320	1.4×10^{-3}	271
Leu	3.6×10^{-1}	180	4.7×10^{-4}	420
Lys	4.0	280	6.1×10^{-4}	315
Ser[b]	8.1×10^{1}	17	8.2×10^{-3}	195
Thr	2.5	280	4.3×10^{-4}	318
Tyr	7.8×10^{-1}	300	1.6×10^{-3}	372

[a] Data were obtained in 25 mM MOPS, 100 mM NaCl, 1 mM dithiothreitol, 5 mM free Mg^{2+}, pH 7.3, at 21 °C in the presence of 10 mM Mg^{2+}-2R,3S-isocitrate or 25 mM Mg^{2+}-2R-malate. Standard errors are less than 20% of estimates.
[b] Wild type.

Detailed kinetics studies show that $K_{m\cdot NADP}$ remains similar to $K_{i\cdot NADP}$ (Fig. 2) for the rapid equilibrium random mechanisms displayed by the wild-type enzyme utilizing 2R-malate and NADP or isocitrate and NAD and for the S113L and S113N enzymes using various combinations of substrate and coenzyme (Dean & Koshland, 1993). The NADP Michaelis constants were shown to be almost identical to the NADP equilibrium dissociation constants of the native enzyme ($K_{d\cdot NADP}$ = 125 μM) and the phosphorylated enzyme ($K_{d\cdot NADP}$ = 141 μM) (Dean et al., 1989). The similarities among the NADP Michaelis constants (Table 1), regardless of the mutation and substrate utilized, suggest that the minor conformational changes induced by substrate binding (Hurley et al., 1990b, 1991; Stoddard et al., 1993) have only small effects on coenzyme binding. Hence, the K_m's accurately reflect thermodynamic dissociation constants.

Performance with isocitrate

Substitution of S113 with alanine breaks the hydrogen bond between the γ-carboxylate of isocitrate and the enzyme, causing performance ($k_{cat}/K_{m\cdot isocitrate}/K_{m\cdot NADP}$) to drop by a factor of 1,000 (Fig. 3). $K_{m\cdot isocitrate}$ is increased by a factor of 3 (Table 2) and k_{cat} reduced by a factor of 30 (Table 3), suggesting that the hydrogen bond plays a minor role in binding isocitrate, even though it plays a major role in promoting catalysis. Similar results are obtained when asparagine and threonine are substi-

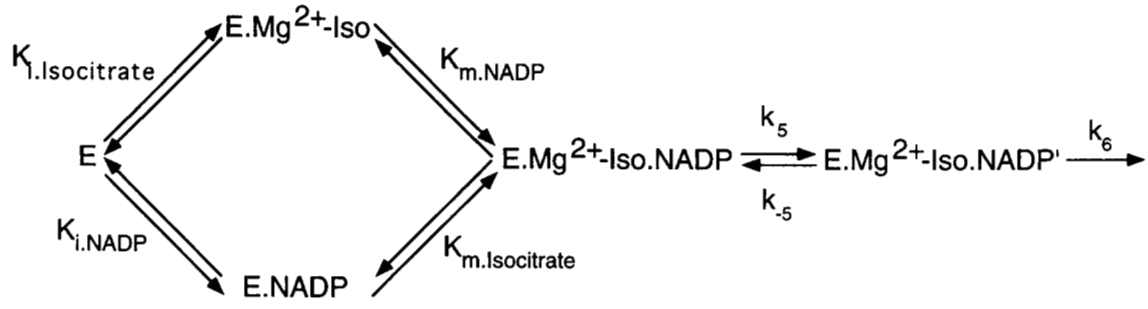

Fig. 2. Steady-state random mechanism of IDH. Steps k_5 and k_{-5} represent alignment of the nicotinamide ring, and k_6 represents steps in catalysis. Catalysis by the wild-type S113 enzyme is sufficiently fast that the kinetic mechanism is steady state, forcing the kinetic estimate of the NADP dissociation constant, $K_{i\cdot NADP} = 17\ \mu M$, to become considerably smaller than that determined from equilibrium binding studies, $K_{d\cdot NADP} = 125\ \mu M$. However, the kinetic estimate of the isocitrate dissociation constant, $K_{i\cdot isocitrate} = 4\ \mu M$, remains similar to its equilibrium dissociation constant, $K_{d\cdot isocitrate} = 5\ \mu M$ (Dean et al., 1989; Dean & Koshland, 1993).

tuted, suggesting that if hydrogen bonds are reestablished, they no longer have the same effect on catalysis.

Specificity toward isocitrate gradually declines as amino acid side-chain volume is increased (Fig. 3). The general trend is caused largely by increases in the Michaelis constants (Table 2), although modest reductions in maximum velocity are also apparent (Table 3). These effects might be due to minor distortions of the active site, steric interactions with the γ-carboxylate of isocitrate, or increasing hydrophobicity inhibiting desolvation of the charged γ-carboxylate at the protein surface.

Figure 3 also illustrates the dramatic reduction in performance caused when the acidic amino acids are introduced at site 113, by factors of 7,650 for aspartate (compared to asparagine) and 1,550 for glutamate (compared to glutamine). The reductions in performance, which affect both $K_{m\cdot isocitrate}$ and k_{cat}, are caused by the electrostatic repulsion of the γ-carboxylate of isocitrate by the negatively charged side chains of aspartate and glutamate (Hurley et al., 1990a, 1990b). This electrostatic effect is

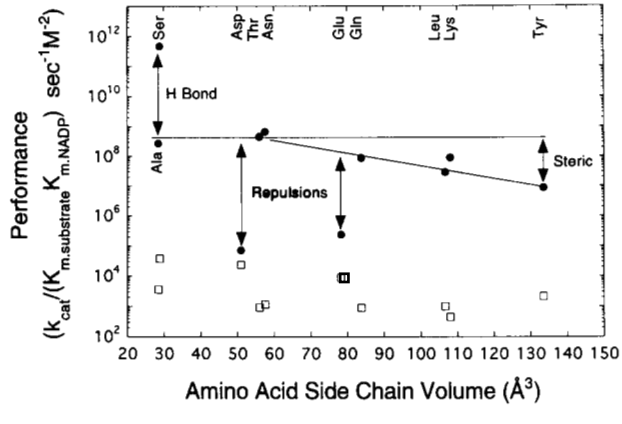

Fig. 3. Specificities of mutant enzymes. The performance factors ($k_{cat}/K_{m\cdot substrate}$) of the various mutant enzymes toward isocitrate (●) and ethanalmalate (□) have been plotted as a function of amino acid side-chain volume. The steric effect and the electrostatic repulsions seen using isocitrate as the substrate are absent when ethanalmalate is used. Note that the performance factors of the aspartate and glutamate mutants toward isocitrate and ethanalmalate are similar, suggesting that isocitrate is protonated on the γ-carboxylate when bound to these mutants.

completely absent when alternative substrates lacking a charged γ-moiety are utilized (Dean & Koshland, 1990).

A homologous series

The γ-moieties of malate (-H), methylmalate ($-CH_3$), ethylmalate ($-CH_2CH_3$), allylmalate ($-CH_2CHCH_2$), and propylmalate ($-CH_2CH_2CH_3$) form a homologous series. For each substrate, neither the maximum velocities nor the Michaelis constants are correlated with amino acid side-chain volume, which is surprising given the results with isocitrate and increasing side-chain volume and the likelihood that the larger γ-moieties probably lie in close proximity to the larger amino acid side chains and the nicotinamide ring during catalysis.

The addition of a methyl group at the 3S position of 2R-malate reduces the Michaelis constant by a factor of 15 for both wild-type and mutant enzymes (Table 2). The further addition of methylenes to the γ-moiety has no discernible effect on the Michaelis constant. Intriguingly, the Michaelis constant toward methylmalate provides an excellent predictor of the Michaelis constant toward the ethyl, allyl, and propyl derivatives (Fig. 4A). Indeed, the Michaelis constants are more characteristic of the individual mutant enzymes than of these substrates.

A similar plot shows that the maximum velocities are correlated but have more scatter (Fig. 4B). As illustrated in Figure 5, there is an optimum volume that maximizes k_{cat} and that roughly corresponds to an ethyl group. The addition of a methyl or ethyl moiety at the 3S position may help align 2R-malate for catalysis and may provide a hydrophobic surface to help align the nicotinamide ring and/or enhance catalysis by excluding solvent. The average k_{cat} with propylmalate is somewhat reduced, as if the size of the γ-moiety has become so great that it distorts the alignments of either substrate, coenzyme, or both.

Hydrophilic γ-moieties

As with the hydrophobic series, the Michaelis constants and maximum velocities with tartrate, ethanolmalate, and ethanalmalate are not correlated with amino acid side-chain volume. Hence, the trends observed with the isocitrate are not reestablished by terminal polar groups at the termini of the γ-moieties. The Michaelis constants and maximum velocities of tartrate are

Table 2. *Mg^{2+}-substrate Michaelis constants*[a]

Residue at site 113	Substrate Michaelis constant (μM)								
	Malate	Methylmalate	Ethylmalate	Propylmalate	Allylmalate	Tartrate	Ethanolmalate	Ethanalmalate	Isocitrate
Ala	1,300	70	70	70	70	80	260	450	30
Asn	2,600	190	150	170	130	90	220	470	20
Asp	1,000	50	40	40	30	30	110	170	1,750
Gln	1,600	100	100	130	100	80	130	310	50
Glu	600	40	40	50	50	40	170	550	700
Leu	1,100	80	70	80	60	60	100	360	70
Lys	4,300	300	290	380	280	120	350	190	160
Ser[b]	1,100	90	100	150	140	50	80	190	10
Thr	1,500	180	150	250	160	90	170	370	20
Tyr	2,000	200	170	160	100	180	530	250	300

[a] Data were obtained in 25 mM MOPS, 100 mM NaCl, 1 mM dithiothreitol, 5 mM free Mg^{2+}, 5 mM NADP, pH 7.3, at 21 °C. Values are the geometric means of estimates obtained from weighted nonlinear least-squares regressions. Standard errors are less than 10% of estimates.
[b] Wild type.

correlated with those of methylmalate (Table 2). The actual values differ, presumably as a consequence of the chemical properties of a hydroxyl versus a methyl at the 3S position. No obvious correlations are seen with ethanolmalate and ethanalmalate, suggesting that the increased hydrophilicity at the termini of the larger γ-moieties begins to obscure the effects seen for the hydrophobic γ-moieties. The possibility that both ethanolmalate and the hydrated form of ethanalmalate hydrogen bond internally may be the reason that their Michaelis constants tend to be higher than those of the hydrophobic series.

The S113E and S113D mutants

A comparison of the kinetics with isocitrate and ethanalmalate (Fig. 3) suggests that the negative charge of the γ-carboxylate of isocitrate contributes greatly to specificity, even in the absence of the hydrogen bond to S113. This suggests that the acidic side chains of the S113D and S113E mutants might enhance the specificity of IDH toward substrates with uncharged γ-moieties. The results are illustrated in Figure 6, where the $\log_{10}$ ratios of the performances of enzymes with charged and uncharged side chains (S113D/S113N and S113E/S113Q) are plotted against the volumes of the uncharged γ-moieties. Positive deviations indicate that the presence of a negative charge in the region enhances specificity toward these substrates. Indeed, a maximum 30-fold increase is seen with the S113D mutant compared with the S113N mutant toward 2R-malate, although this gradually diminishes as the volume of the γ-moiety increases. The S113D mutant also appears rather more active toward ethanolmalate than the S113N mutant. The data with the S113E mutant show a similar trend, although the data are more scattered.

Discussion

The large number of permutations developed by combining nine different substrates with 10 different enzymes provides some in-

Table 3. *Maximum velocities*[a]

Residue at site 113	Maximum velocity (s^{-1})								
	Malate	Methylmalate	Ethylmalate	Propylmalate	Allylmalate	Tartrate	Ethanolmalate	Ethanalmalate	Isocitrate
Ala	1.2×10^{-3}	2.2×10^{-2}	2.2×10^{-2}	1.0×10^{-2}	4.4×10^{-2}	1.4×10^{-3}	3.7×10^{-2}	3.7×10^{-2}	2.2
Asn	6.9×10^{-4}	1.8×10^{-2}	4.2×10^{-2}	1.7×10^{-2}	3.0×10^{-2}	8.6×10^{-4}	5.3×10^{-3}	1.2×10^{-2}	3.8
Asp	7.6×10^{-3}	6.2×10^{-2}	6.1×10^{-2}	1.8×10^{-2}	1.9×10^{-2}	6.4×10^{-3}	9.3×10^{-2}	1.6×10^{-2}	3.3×10^{-2}
Gln	4.1×10^{-4}	1.3×10^{-2}	2.4×10^{-2}	1.3×10^{-2}	5.1×10^{-2}	7.2×10^{-4}	9.0×10^{-3}	1.4×10^{-2}	1.0
Glu	1.4×10^{-3}	4.7×10^{-2}	1.3×10^{-1}	4.7×10^{-2}	5.6×10^{-2}	1.4×10^{-3}	4.8×10^{-2}	3.9×10^{-2}	5.3×10^{-2}
Leu	4.6×10^{-4}	1.5×10^{-2}	8.0×10^{-2}	1.3×10^{-2}	5.1×10^{-2}	8.0×10^{-4}	4.3×10^{-3}	4.2×10^{-2}	3.5×10^{-1}
Lys	6.1×10^{-4}	4.8×10^{-2}	8.6×10^{-2}	3.4×10^{-2}	6.9×10^{-2}	1.6×10^{-3}	3.1×10^{-2}	1.3×10^{-2}	4.0
Ser[b]	8.1×10^{-3}	3.0×10^{-2}	5.6×10^{-2}	2.9×10^{-2}	7.4×10^{-2}	1.1×10^{-2}	4.8×10^{-2}	1.9×10^{-2}	7.9×10^{1}
Thr	4.3×10^{-4}	2.0×10^{-2}	3.6×10^{-2}	2.2×10^{-2}	5.3×10^{-2}	8.8×10^{-4}	6.8×10^{-3}	1.3×10^{-2}	2.5
Tyr	1.6×10^{-3}	5.7×10^{-2}	5.0×10^{-1}	1.7×10^{-1}	3.3×10^{-1}	6.0×10^{-3}	5.9×10^{-2}	5.4×10^{-2}	7.8×10^{-1}

[a] Data were obtained in 25 mM MOPS, 100 mM NaCl, 1 mM dithiothreitol, 5 mM free Mg^{2+}, 5 mM NADP, pH 7.3, at 21 °C. Values are the geometric means of estimates obtained from weighted nonlinear least-squares regressions. Standard errors are less than 15% of estimates.
[b] Wild type.

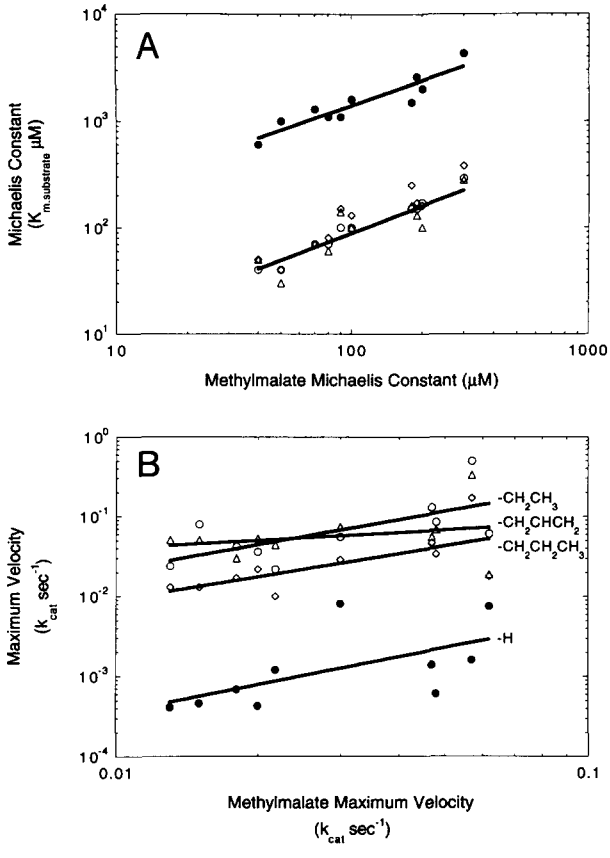

Fig. 4. Correlations among the kinetic constants for each mutant enzyme with substrates having hydrophobic γ-moieties. **A:** The substrate Michaelis constants of each enzyme are plotted against the methylmalate Michaelis constant of each enzyme. The strong correlation, retained with 2R-malate, suggests that interactions between the γ-moieties and amino acid residues at site 113 are weak. **B:** A similar plot for the maximum velocities reveals more scatter, although the general trend is still apparent. ●, Malate; △, methylmalate; ○, ethylmalate; ◇, allylmalate; □, propylmalate.

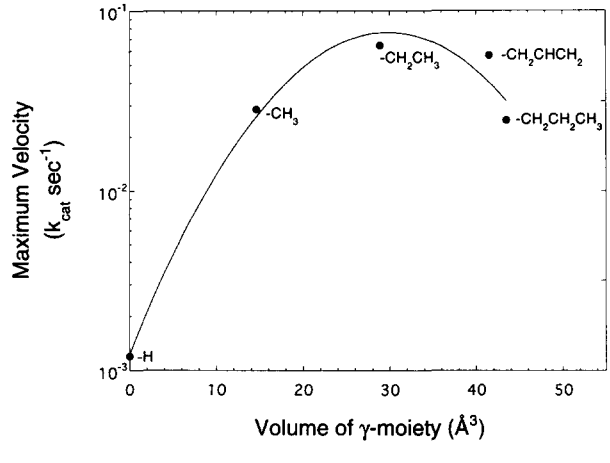

Fig. 5. Effect of γ-moiety volume on k_{cat} for the series of hydrophobic γ-moieties. Volumes were determined using the protein comparison package available in Quanta™. The curve is a nonlinear least-squares fit to a second-order polynomial.

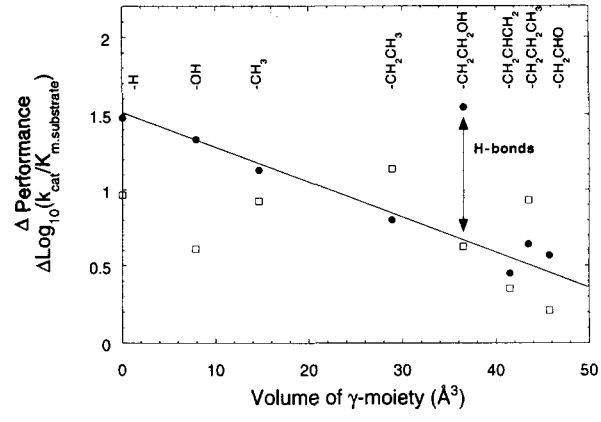

Fig. 6. Effect of a negative charges on performance factors toward analogues with uncharged γ-moieties. The positive difference between the logged performance factors ($\Delta \log_{10}(k_{cat}/K_m) = \log_{10}(k_{cat\cdot 1}/K_{m\cdot 1}) - \log_{10}(k_{cat\cdot 2}/K_{m\cdot 2}) = \log_{10}[(k_{cat\cdot 1}/K_{m\cdot 1})/(k_{cat\cdot 2}/K_{m\cdot 2})]$) of the S113D and S113N mutants (●) and the S113E and S113Q mutants (□) suggests that the introduction of a negative charge at site 113 enhances specificity when the γ-moieties of the substrates are uncharged. Volumes were determined using the protein comparison package available in Quanta™.

sight into the determinants of specificity in this enzymatic reaction. As an objective assessment of specificity, we have used the parameter $k_{cat}/K_{m\cdot substrate}/K_{m\cdot NADP}$, which we call the performance factor, because it measures the parameter involved in developing an effective enzyme in the linear region of the velocity versus [*S*] plot.

The addition of a methyl moiety at the 3S position of 2R-malate raises performance by a factor of 45 (Fig. 7). A second methyl moiety in ethylmalate further raises the performance by a factor of 1.7. However, a third methyl moiety reduces performance by a factor of 0.35, suggesting that the site becomes a little too crowded in the case of propylmalate. The performance with allylmalate is 2.7 times higher than with propylmalate, indicating that a modest reduction substrate volume can noticeably improve performance. The addition of polar hydroxyl groups, for example from ethyl to ethanol, has relatively little

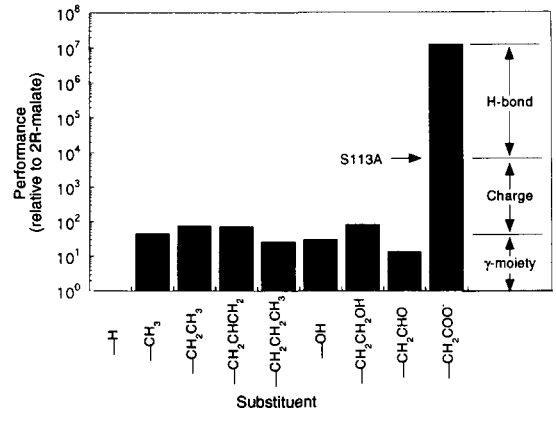

Fig. 7. Partitioning the contributions to specificity made by the γ-moiety of isocitrate for the wild-type enzyme. Data are from Tables 1, 2, and 3.

effect on performance (Fig. 7). Overall, the changes in performance achieved by additional methyl groups and polar hydroxyl groups are relatively small.

Replacing the serine at position 113 by other amino acids has relatively little effect on these trends. However, the mutant enzymes reveal an intriguing phenomenon (Fig. 4A). The substrate Michaelis constant toward methylmalate provides an excellent predictor of the Michaelis constant toward the ethyl, allyl, and propyl derivatives. The correlation remains with 2R-malate, suggesting that amino acid substitutions at site 113 affect binding, not through direct interactions with the γ-moieties of the substrates, but indirectly, perhaps by affecting solvent electrostatics or inducing subtle conformational changes in the 2R-malate part of the binding site.

The introduction of a carboxylate on the γ-moiety of the substrate contributes an enormous factor of 250,000 to performance. Of this, 1,650 can be ascribed to formation of a hydrogen bond with S113, leaving 150, which can be ascribed to the negative charge. These results are fully in accord with X-ray structures of the ternary complex (Stoddard et al., 1993), showing that the nicotinamide mononucleotide moiety of NADP makes few contacts with the enzyme and is stabilized by a salt bridge from the nicotinamide ring to the γ-carboxylate of bound isocitrate. Hence, the γ-carboxylate of bound isocitrate, which forms the binding site for the nicotinamide ring, is a key determinant of performance.

That the negative charge of the γ-carboxylate plays a key role in determining performance receives further support from the S113D and S113E mutants. When utilizing the synthetic substrates, S113D is more active than S113N, and S113E is more active than S113Q. These results suggest that the introduction of negatively charged side chains in the general vicinity of position 113 can also stabilize the nicotinamide ring in a manner reminiscent of the γ-carboxylate of bound isocitrate.

Interestingly, the performance of the S113D enzyme progressively diminishes as the size of the γ-moieties is increased, perhaps because larger γ-moieties physically intercede between the negative carboxylate and the positive nicotinamide ring. The sole exception to the trend is provided by ethanolmalate. Conceivably, the terminal hydroxyl of this substrate might bridge the aspartate carboxylate and the nicotinamide ring, again enhancing specificity. Ethanalmalate shows no evidence of enhanced specificity, suggesting that subtle differences in structure can have surprisingly marked effects. The S113E mutant shows the same general trend, but the data are more scattered, perhaps because of the greater conformational flexibility of its side chain.

Both enzymes display higher specificities toward the synthetic substrates, up to 80-fold with ethylmalate, than toward isocitrate. Hence, the specificities of these mutants are inverted.

Materials and methods

Materials

Strains, growth conditions, site-specific mutagenesis, enzyme purification, and protein determinations have been described previously (Dean et al., 1989; Dean & Koshland, 1990). Dimethyl 2R-malate was obtained from Fluka, and thionyl chloride came from Fisher. 2R-malate, ethyl iodide, methyl iodide, and allyl bromide were obtained from Aldrich.

Syntheses

Diethyl 2R-malate was prepared from 2R-malate and ethanol in the presence thionyl chloride using standard procedures (Miller et al., 1982). Diesterified 2R-malate derivatives (dimethyl (2R,3S)-3-methylmalate, dimethyl (2R,3S)-3-ethylmalate, and diethyl (2R,3S)-3-allylmalate) were prepared by diastereoselective alkylation of the appropriate 2R-malate alkoxide enolates according to the method of Seebach (Wasmuth et al., 1982; Seebach et al., 1985). Diethyl (2R,3S)-3-propylmalate was obtained from diethyl (2R,3S)-3-allylmalate by hydrogenation over palladium on charcoal (catalytic) in methanol at room temperature. Treatment of diethyl (2R,3S)-3-allylmalate in 1:4 H_2O/dioxane with $NaIO_4$ (~5 equivalents) and OsO_4 (catalytic) afforded diethyl (2R,3S)-3-ethanalmalate. Diethyl (2R,3S)-3-ethanolmalate was prepared from diethyl (2R,3S)-3-ethanalmalate in methanol in the presence of sodium borohydride. The various diesters were purified by chromatography over silica gel. The diacids were obtained by hydrolysis of the corresponding diesters by treatment with LiOH (3 equivalents) in 1:1 THF/H_2O at room temperature followed by elution through H+ resin (Dowex 50W; SO_3H). (2R,3S)-3-ethylmalate was recrystallized from ethyl ether at −20 °C. All compounds were at least 90% diastereomerically pure as determined from ^1H NMR spectra in D_2O. The purity of 2R,3S-ethanolmalate was not determined.

Kinetics assays

The kinetics of the enzymes were determined in 25 mM MOPS, 100 mM NaCl, 1 mM dithiothreitol, pH 7.3, at 21 °C in the presence of 5 mM free Mg^{2+}. The quantities of $MgCl_2$ added to bring the concentration of free Mg^{2+} to 5 mM were calculated using the equilibrium dissociation constants of the Mg^{2+}-substrate and Mg^{2+}-NADP complexes presented in Table 4, which were determined using 8-hydroxyquinoline by the method of Burton (1959). Data were collected on a Hewlett-Packard

Table 4. *Dissociation constants of Mg^{2+}-ligand complexes*[a]

		Published values	
Ligand	pK_d	pK_d	Source
Malate	1.6	1.6	Dawson et al. (1969)
Methylmalate	1.5		
Ethylmalate	1.6		
Propylmalate		1.5	
Allylmalate	1.5		
Tartrate	1.4	1.4	Dawson et al. (1969)
Ethanolmalate	1.7		
Ethanalmalate	1.6		
Isocitrate	2.1	3.2	Duggleby and Dennis (1970)
		2.3	Northrop and Cleland (1974)
		3.1	Willson and Tipton (1981)
		2.2	Grissom and Cleland (1988)
NADP	3.0	1.7	Apps (1973)

[a] Data were obtained in 25 mM MOPS, 100 mM NaCl, 1 mM dithiothreitol, 1 mM 8-hydroxyquinoline, pH 7.3, at 21 °C. $pK_d = -\log_{10}$([free ligand][free enzyme]/[bound ligand]). Standard errors are less than 15% of the estimates.

8452A single beam diode array spectrophotometer, which is capable of measuring reaction rates as low as 6×10^{-6} Δ_{340nm}/30 min using repeated blanking with internal referencing at 440 nm. The rates of reaction were determined by monitoring the production of NADPH at 340 nm in a 1-cm light path. The concentration of NADPH was determined using a molar extinction coefficient of 6,200 Δ_{340nm}/cm. Protein concentrations were determined at 280 nm using a molar extinction coefficient of 66,330 Δ_{280nm}/cm (Dean et al., 1989).

Analysis

Weighted nonlinear least-squares regressions were used to estimate V_{max} and K_m of the Michaelis-Menten equation. The performance of the enzymes in the various assays was evaluated by the term $k_{cat}/K_{m\cdot isocitrate}/K_{m\cdot NADP}$, where the K_m's had previously been determined to be equal to the true thermodynamic dissociation constants (Dean & Koshland, 1993). This term, which we call the performance factor, is an extension of the usual k_{cat}/K_m to a bisubstrate reaction.

Acknowledgments

This work was supported by the Lucille P. Markey Charitable Trust and the National Science Foundation (grant 04200 to D.E.K.) and the National Institutes of Health (grant GM-48735 to A.M.D.). We thank David Benson and Peter Schultz for assistance with the organic synthesis and characterization of the compounds.

References

Apps DK. 1973. Complex formation between magnesium ions and pyridine nucleotide coenzymes. *Biochim Biophys Acta 320*:379–387.

Bolduc JM, Dyer DM, Scott WG, Singer P, Sweet RM, Koshland DE Jr, Stoddard BL. 1995. The use of mutagenesis & Laue crystallography to examine the intermediates in a reaction pathway: Isocitrate dehydrogenase. *Science 268*:1312–1318.

Borthwick AC, Holms WH, Nimmo HG. 1984. Amino acid sequence around the site of phosphorylation in isocitrate dehydrogenase from *Escherichia coli* ML308. *FEBS Lett 174*:112–115.

Burton K. 1959. Formation constants for the complexes of adenosine di- and tri-phosphates with magnesium or calcium. *Biochem J 71*:388–395.

Dawson RMC, Elliot DC, Elliot WH, Jones KM. 1969. *Data for biochemical research, 2nd ed.* Oxford, UK: Clarendon Press.

Dean AM, Koshland DE Jr. 1990. Electrostatic and steric contributions to regulation at the active site of isocitrate dehydrogenase. *Science 249*: 1044–1046.

Dean AM, Koshland DE Jr. 1993. The kinetic mechanism of *Escherichia coli* isocitrate dehydrogenase. *Biochemistry 32*:9302–9309.

Dean AM, Lee MHI, Koshland DE Jr. 1989. Phosphorylation inactivates *Escherichia coli* isocitrate dehydrogenase by preventing isocitrate binding. *J Biol Chem 264*:20482–20486.

Duggleby RG, Dennis DT. 1970. Nicotinamide adenine dinucleotide-specific isocitrate dehydrogenase from a higher plant. *J Biol Chem 245*:3745–3754.

Ehrlich RS, Colman RF. 1987. Ionization of isocitrate bound to pig heart $NADP^+$-dependent isocitrate dehydrogenase. ^{13}C NMR study of substrate binding. *Biochemistry 26*:2461–2471.

Grissom CB, Cleland WW. 1988. Isotope effect studies of the chemical mechanism of pig heart NADP isocitrate dehydrogenase. *Biochemistry 27*:2934–2943.

Hurley JH, Dean AM, Koshland DE Jr, Stroud RM. 1991. Catalytic mechanism of $NADP^+$-dependent isocitrate dehydrogenase: Implications from the structures of magnesium-isocitrate and $NADP^+$ complexes. *Biochemistry 30*:8671–8678.

Hurley JH, Dean AM, Stohl JL, Koshland DE Jr, Stroud RM. 1990a. Regulation of an enzyme by phosphorylation at the active site. *Science 249*:1012–1016.

Hurley JH, Dean AM, Thorsness PE, Koshland DE Jr, Stroud RM. 1990b. Regulation of isocitrate dehydrogenase by phosphorylation involves no long-range conformational change in the free enzyme. *J Biol Chem 265*:3599–3602.

Hurley JH, Thorsness P, Ramalingham V, Helmers N, Koshland DE Jr, Stroud RM. 1989. Structure of a bacterial enzyme regulated by phosphorylation, isocitrate dehydrogenase. *Proc Natl Acad Sci USA 86*:8635–8639.

Miller MJ, Bajwa JS, Mattingly PG, Peterson K. 1982. Enantioselective synthesis of 3-substituted 4-(alkoxycarbonyl)-2-azetidinones from malic acid. *J Org Chem 47*:4928–4933.

Northrop DB, Cleland WW. 1974. The kinetics of pig heart triphosphopyridine nucleotide-isocitrate dehydrogenase. *J Biol Chem 249*:2928–2931.

Seebach D, Aebi J, Wasmuth D. 1985. Diastereoselective α-alkylation of β hydroxycarboxylic esters through alkoxide enolates: (+)-Diethyl (2S,3R)-3-allyl-2-hydroxysuccinate from (−)-diethyl *S*-malate. *Organ Synth 63*:109–120.

Stoddard BL, Dean AM, Koshland DE Jr. 1993. Structure of isocitrate dehydrogenase with isocitrate, nicotinamide adenine dinucleotide phosphate, and calcium at 2.5-Å resolution: A pseudo-Michaelis ternary complex. *Biochemistry 32*:9310–9316.

Thorsness PE, Koshland DE Jr. 1987. Inactivation of isocitrate dehydrogenase by phosphorylation is mediated by the negative charge of the phosphate. *J Biol Chem 262*:10422–10425.

Wasmuth D, Arigoni D, Seebach D. 1982. Zum stereochemischen Verlauf der Biosynthese von 2-Oxo-pantolacton: Synthese von stereospezifisch indiziertem Pantolacton aus Äpfelsaure. *Helv Chim Acta 65*:344–352.

Willson VJC, Tipton KF. 1981. The activation of ox-brain NAD^+-dependent isocitrate dehydrogenase by magnesium ions. *Eur J Biochem 113*:477–483.